

# Influence of initial charge conditions on engine performance and emission of a DISI hydrogen-fueled engine under various injection timings

Vahid FATHI<sup>1,\*</sup>, Arash NEMATI<sup>2</sup>, Samad JAFARMADAR<sup>1</sup>  
Shahram KHALILARYA<sup>1</sup>

<sup>1</sup>*Mechanical Engineering Department, Technical Education Faculty, Urmia University, Urmia, West Azerbaijan-IRAN  
e-mail: nemati.fathi@gmail.com*

<sup>2</sup>*Mechanical Engineering Department, Miyaneh Branch, Islamic Azad University, Miyaneh-IRAN*

Received: 27.10.2010

## Abstract

Using hydrogen as an alternative fuel in spark-ignition engines has great potential for reducing exhaust emissions. Hydrogen engines have CO<sub>2</sub>- and HC-free combustion and lean operation, offering lower nitrogen oxide (NO<sub>x</sub>) emission. In this paper, a numerical study of a direct injection spark-ignition (DISI) hydrogen-fueled engine was conducted via 3-dimensional computational fluid dynamics (CFD) methods and results were compared with experimental data, showing good agreement. Injection timing, initial charge temperature, and initial charge pressure were selected as effective and controllable parameters of emissions and performance characteristics. Results showed that mixture homogeneity was more affected by injection timing, and advancing the injection timing led to improved engine performance with a slight increase in NO<sub>x</sub> emissions. Increasing the initial pressure and decreasing the initial temperature led to better engine performance and reduced NO<sub>x</sub> emissions in the DISI hydrogen-fueled engine.

**Key Words:** Hydrogen engine, DISI, initial condition, NO<sub>x</sub> emission

## 1. Introduction

Hydrogen has been regarded as a future alternative fuel for power systems due to its CO<sub>2</sub>- and HC-free operation. Recent drastic increases in the price of petroleum, rapid increases in the emission of greenhouse gases, and very strict environmental legislation are major motivating factors for the usage of hydrogen in fuel cells and internal combustion engines (Room, 2006). Hydrogen internal combustion engines have the ability to increase efficiency (Tang et al., 2002). Many researchers have investigated hydrogen engine characteristics. These studies state that hydrogen internal combustion engines have a high efficiency, along with being very clean and considerably cheaper than fuel cells (Verhelst et al., 2006). Hydrogen has unique combustion characteristics that are different from those of gasoline, and it needs some special attention when it is employed in an engine. The laminar flame

---

\*Corresponding author

speed of a hydrogen-air mixture at stoichiometric conditions is about 10 times that of gasoline. The wide flammability limit of hydrogen allows for the use of very low equivalence ratios, which result in reduced  $\text{NO}_x$  emissions. The 106 RON octane rating of hydrogen allows for an increased compression ratio (Verhelst and Wallner, 2009). Hydrogen fuel delivery systems can be considered as belonging to 3 main types: carbureted injection, port fuel injection (PFI), and direct injection (DI) (Rahman et al., 2009). For hydrogen spark-ignition engines, there are 3 regimes of abnormal combustion: knock (autoignition of the end-gas region), preignition (uncontrolled ignition induced by a hot spot, premature to the spark ignition), and backfire (also referred to as backflash, flashback, and induction ignition, this is a premature ignition during the intake stroke, which could be seen as an early form of preignition) (Sierens et al., 2005). Efforts to avoid combustion anomalies and increase the power density of hydrogen internal combustion engines while achieving near-zero emissions have led to the development of injection systems for hydrogen DI operation (Verhelst et al., 2006). Similar to common classifications for gasoline direct injection (GDI) engines, hydrogen DI mixture formation strategies have also been grouped into jet-guided, wall-guided, and air-guided concepts (Kirchweger et al., 2006). DI injection can be classified as early DI and late DI based on the start of injection. Early injection generally refers to any hydrogen DI during the early compression stroke, shortly after the closing of the intake valve, whereas late DI refers to strategies with the injection late in the compression stroke, generally ending just before spark timing (Verhelst et al., 2006).

Kovac et al. (2005) used 3-dimensional computational fluid dynamics (CFD) simulations to investigate the influence of injection timing on mixture formation and combustion characteristics. They concluded that, with early injection, the injected hydrogen has enough time to mix with the air inside the combustion chamber and form a homogeneous mixture, while, in late injection, there is not sufficient time for mixing, resulting in a stratified charge at spark timing. Kaiser and White (2008) demonstrated this phenomenon with optically accessible engines. The effect of injection timing on  $\text{NO}_x$  emission formation under various equivalence ratios was presented by Wallner et al. (2006, 2007). Salazar et al. (2009) have shown that at low engine loads, early injection results in extremely low  $\text{NO}_x$  emissions because the mixture at ignition timing is very likely to be homogeneous. Thus, the lean homogeneous mixture burns without forming  $\text{NO}_x$  emissions. Late injection at low loads, on the other hand, results in a stratified mixture with hydrogen-rich zones, as well as zones with very lean mixtures or even pure air. Although the overall mixture is still lean, the combustion of the rich zones causes a significant increase in  $\text{NO}_x$  emissions. At high engine loads, this trend appears to be inverted. Early injection results in homogeneous mixtures that approach stoichiometry and produce high  $\text{NO}_x$  emissions. Late injection is expected to result in stratification, with zones that are even richer than stoichiometric, along with lean zones. This kind of stratification avoids the  $\text{NO}_x$  critical equivalence ratio regime ( $\lambda \approx 1.3$ ) and thereby reduces overall  $\text{NO}_x$  emissions (Wallner et al., 2006, 2007). Since the air amount remains almost constant with a changing equivalence ratio during the direct injection of  $\text{H}_2$  (the displacement effect is precluded because  $\text{H}_2$  is not injected before the intake valves close), a leaner equivalence ratio under the same load is established as compared with the external mixture formation with  $\text{H}_2$ . Since both  $\text{NO}_x$  emissions and engine efficiency are strongly dependent on the equivalence ratio, DI operation is capable of achieving higher engine efficiencies and lower  $\text{NO}_x$  emissions at the same engine load as compared to port injection (Eichseder et al., 2003).

Wallner et al. (2009) demonstrated that optimization of efficiency with injection configurations in hydrogen DI strategy at low- and part-load conditions as well as at high engine loads led to an increase in the production of  $\text{NO}_x$ . For example, an increase in indicated efficiency from 29% to 34% led to an increase

in  $\text{NO}_x$  emissions from around 5 ppm with early injection to more than 100 ppm. To achieve high engine efficiencies and low  $\text{NO}_x$  emissions, supercharging and exhaust gas recirculation (EGR) have been presented as effective tools. Results from various investigations (Berckmüller et al., 2003; Natkin et al., 2003; Verhelst et al., 2009) suggest that using EGR combined with supercharging has a significant effect on increasing the power output while limiting tailpipe emissions of  $\text{NO}_x$ .

From the above, it is clear that there are a number of operating strategies for hydrogen engines that depend on the power demand and are related to the limitation of  $\text{NO}_x$  emissions. There are also some methods for studying those operating strategies that employ CFD simulation as a powerful and reliable method in predicting engine treatment, and there are a few studies that have investigated the effect of initial charge conditions, simultaneously with various injection timings, on the performance and emission of hydrogen-fueled direct injection spark-ignition (DISI) engines. Therefore, the objective of this study was to use a numerical model to simulate mixture formation and combustion inside a DISI hydrogen-fuelled engine under different initial and injection conditions. Initial charge pressures and temperatures under various injection timings were studied and the results were compared to determine how these parameters affected performance characteristics and  $\text{NO}_x$  emission production.

## 2. Model description

Computer predictions of the performance and emissions of engines would enable cheap and fast engine optimization. In the present study, DISI hydrogen-fuelled engine operation was analyzed by using the AVL FIRE CFD code, which uses a 3D moving mesh for combustion chamber simulation. Figure 1 shows a schematic of the 3D moving mesh at a  $40^\circ$  crank angle (CA) before top dead center (BTDC).

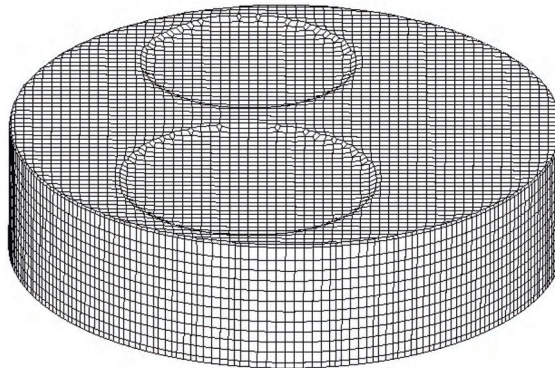


**Figure 1.** 3D moving mesh at  $40^\circ$  CA BTDC.

The numerical model for a single cylinder, 4-stroke, natural aspirated SI engine, which was converted from a direct injection diesel engine (Yanmar NFD-170) (Mohammadi et al., 2007), was used to evaluate engine operating characteristics. In this engine, a flat-head piston was used to form the disk-shaped combustion space, and hydrogen gas was injected into the combustion chamber with a gas injector. The distance between the spark plug and injection nozzle tip was approximately 30 mm. The other engine specifications are listed in the Table.

Calculations were carried out on a closed system from intake valve closing time (IVC) at a  $-140^\circ$  CA to exhaust valve opening time (EVO) at a  $130^\circ$  CA. The grid was generated to model the geometry of the

**Table.** Engine specifications.

Engine type	Spark-ignition 4-stroke cycle
Engine speed	1200 rpm
Bore $\times$ stroke	102 mm $\times$ 105 mm
Displacement volume	857 cc
Compression ratio	11.5:1
Swirl ratio	2.6
Injector nozzle	0.52 mm $\times$ 7
Combustion chamber	Disk-shaped

engine and contained a maximum of 73,246 cells at a 130° CA BTDC. Different grid densities were tested prior to the study, and the present resolution was found to give adequately grid-independent results with a reasonable CPU run time. The AVL FIRE code solves the compressible, turbulent, 3-dimensional transient conservation equations for reacting multicomponent gas mixtures. The turbulent flow within the combustion chamber is simulated using the RNG  $k - \varepsilon$  turbulence model, modified for variable-density engine flows (Han and Reitz, 1995), considered to be one of the suitable turbulence models for engine simulation studies. Initial conditions for turbulence kinetic energy (TKE) and turbulence length scale (TLS) were calculated according to the formulation provided in the AVL FIRE User Manual (2006) and described below:

$$TKE = (3/2) \times u'^2, \quad (1)$$

$$u' = 0.25 \times (2 \times S \times (N/60)). \quad (2)$$

In the above equations,  $u'$  is the turbulent fluctuation velocity (m/s),  $S$  is the stroke (m), and  $N$  is the engine speed.

$$TLS = h_v/2, \quad (3)$$

where  $h_v$  is the maximum valve lift (m).

The combustion process is modeled by the eddy-breakup model. The burning zone consists of parcels of burned gas and almost fully burned gas. The intrinsic idea behind the eddy-breakup model is that the rate of combustion is determined by the rate at which parcels of unburned gas are broken down into smaller ones, such that there is sufficient interfacial area between the unburned mixture and hot gases to permit a reaction (Bray, 1980). The rate of dissipation of these eddies determines the rate of combustion:

$$\frac{\dot{r}_{fu}}{\bar{\rho}} = \frac{C_{fu}}{\tau_R} \bar{\rho} \min \left( \bar{y}_{fu}, \frac{\bar{y}_{ox}}{S}, \frac{C_{pr} \cdot \bar{y}_{pr}}{1 + S} \right). \quad (4)$$

The first 2 terms of the “minimum value of” operator determine whether fuel or oxygen is present in limiting quantities, and the third term is a reaction probability that ensures that the flame is not spread in the absence of hot products. This equation includes 3 constant coefficients ( $C_{fu}, \tau_R, C_{pr}$ ), and  $C_{fu}$  varies from 3 to 25. An optimum value was selected according to experimental data (AVL FIRE User Manual, 2006).

The  $NO_x$  formation model is derived by a systematic reduction of multistep chemistry, based on the partial equilibrium assumption of the considered elementary reactions using the extended Zeldovich mechanism (Zeldovich et al., 1974) describing the thermal nitrous oxide formation.



### 3. Model validity

To show the model validation from the first-law perspective, diagrams of the cylinder pressure under 3 injection timings were compared with the experimental data (Mohammadi et al., 2007); they showed very good agreement (Figures 2a-2c).

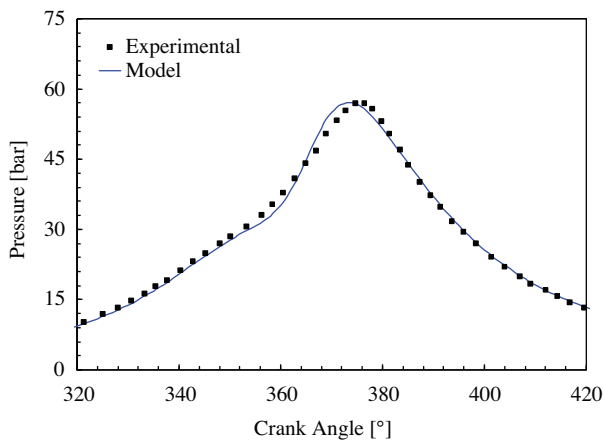


**Figure 2a.** Model validation under injection timing of 130° CA BTDC, spark timing of 11° CA BTDC.

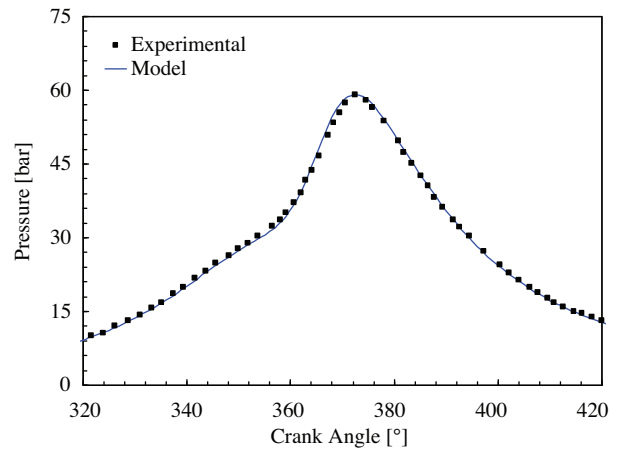


**Figure 2b.** Model validation under injection timing of 100° CA BTDC, spark timing of 11° CA BTDC.

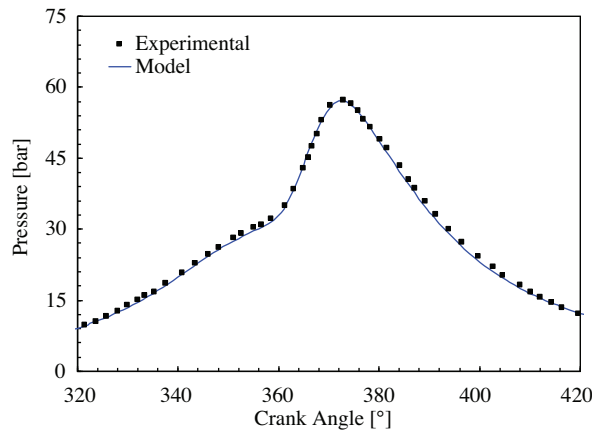


**Figure 2c.** Model validation under injection timing of 80° CA BTDC, spark timing of 8° CA BTDC.

Figure 3 shows the calculated  $NO_x$  emission for injection timing of 130° CA BTDC compared with experimental results. The good agreement between the measured and calculated  $NO_x$  emissions makes the model predictions more reliable and suggests that the model can be used for other simulations.

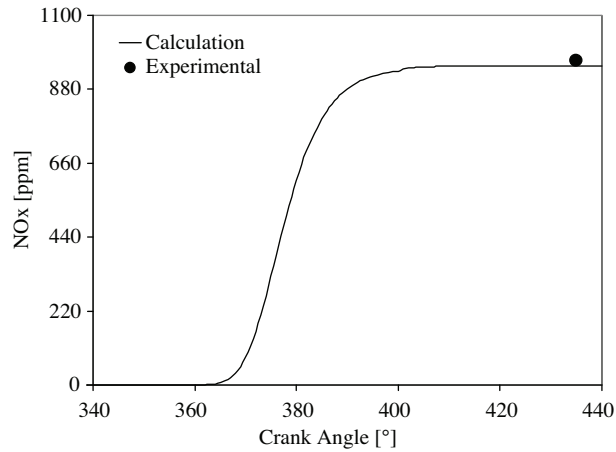


**Figure 3.** Comparison between calculated and measured  $\text{NO}_x$  emission under injection timing of  $130^\circ$  CA BTDC, spark timing of  $11^\circ$  CA BTDC.

## 4. Results

### 4.1. Effect of initial charge temperature

The aim of this section is to investigate the effect of initial charge temperature on the emissions and combustion characteristics under 3 injection timings,  $130^\circ$ ,  $100^\circ$ , and  $80^\circ$  CA BTDC. Therefore, the same conditions for engine speed, swirl ratio, and other initial charge conditions at IVC were used for the simulations.

Predicted in-cylinder pressure and temperature profiles are shown in Figures 4a, 4b, 5a, 5b, 6a, and 6b for injection timings of  $80^\circ$ ,  $100^\circ$ , and  $130^\circ$  CA BTDC, respectively. By comparison of these profiles, it can be understood that by early injection of hydrogen into the cylinder, the air and fuel can mix homogeneously and combustion can occur completely; therefore, the work done per cycle increases. Retarding the hydrogen injection into the combustion chamber results in a decrease in the work done per cycle. This is due to the time needed for air-fuel mixing, which decreases with the retarding of the hydrogen injection such that the air-fuel mixture will be inhomogeneous in the spark timing and deficient combustion will happen. Additionally, a high concentration of hydrogen around the spark plug combustion starts fast and ceases rapidly. In other words, the combustion duration decreases and therefore pressure will be less in the expansion stroke, which results in decreased work. As can be seen, by increasing the initial charge temperature, the maximum in-cylinder pressure is decreased. By increasing the initial charge temperature, the density of inlet mass and the amount of oxygen decrease, leading to deficient combustion and a reduction of maximum in-cylinder pressure. Figures 4b, 5b, and 6b show that increasing the initial charge temperature causes an increase in the temperature level in the cylinder.

Figure 7 indicates the effect of changing the initial charge temperature on the predicted  $\text{NO}_x$  concentration under the various injection timings. There are some important parameters in  $\text{NO}_x$  formation, such as in-cylinder oxygen concentration, the energy that leads to thermal decomposition of oxygen and nitrogen molecules, the time needed for reaction of nitrogen and oxygen atoms depending on engine speed, and the premier parameter in DISI engines, in-cylinder mixture homogeneity at the ignition timing and thus at the time of start of combustion. By increasing the initial charge temperature, the oxygen concentration is decreased and the amount of energy needed for decomposition of  $\text{N}_2$  and  $\text{O}_2$  molecules increases because of the increased

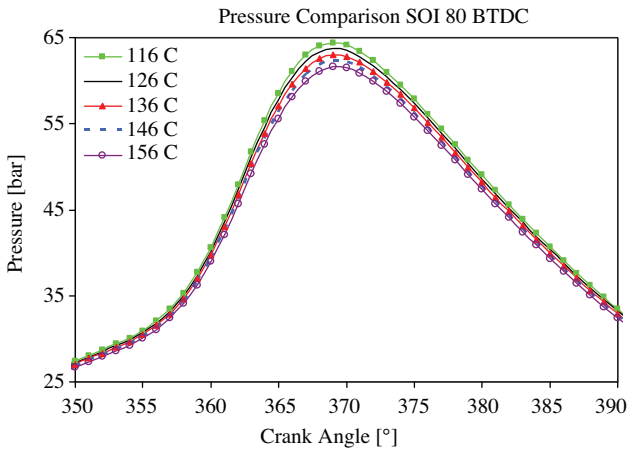


**Figure 4a.** Effect of initial charge temperature on cylinder pressure under injection timing of  $80^\circ$  CA BTDC.

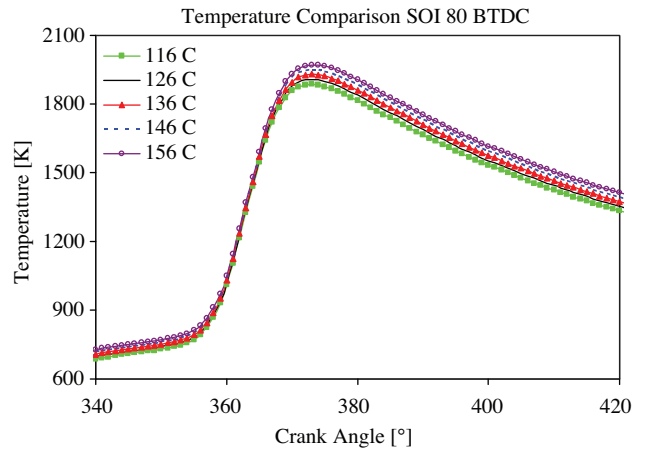


**Figure 4b.** Effect of initial charge temperature on cylinder temperature under injection timing of  $80^\circ$  CA BTDC.

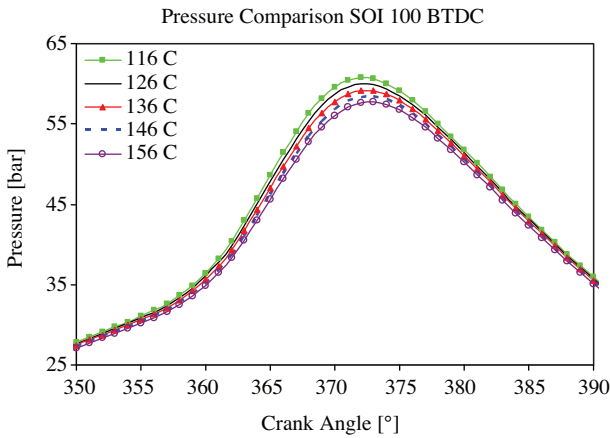


**Figure 5a.** Effect of initial charge temperature on cylinder pressure under injection timing of  $100^\circ$  CA BTDC.

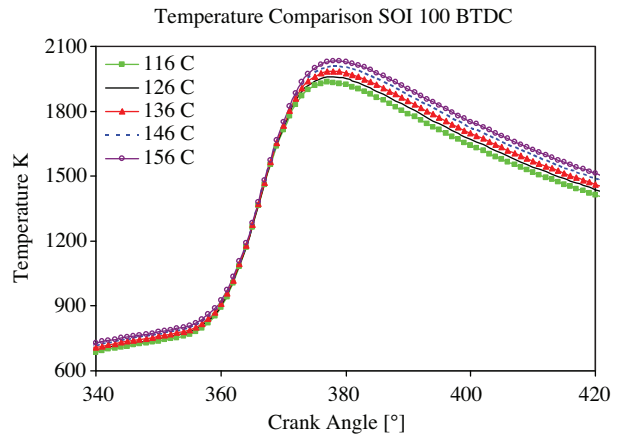


**Figure 5b.** Effect of initial charge temperature on cylinder temperature under injection timing of  $100^\circ$  CA BTDC.

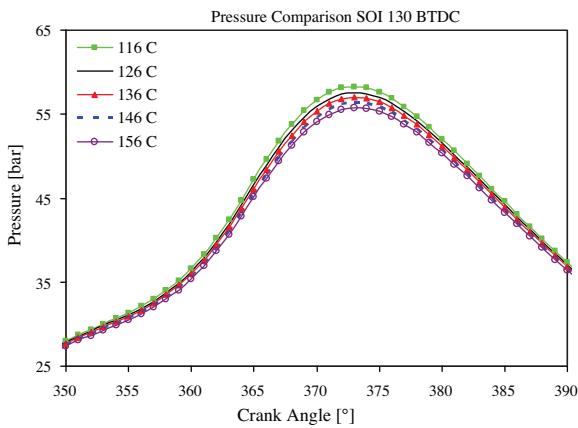


**Figure 6a.** Effect of initial charge temperature on cylinder pressure under injection timing of  $130^\circ$  CA BTDC.

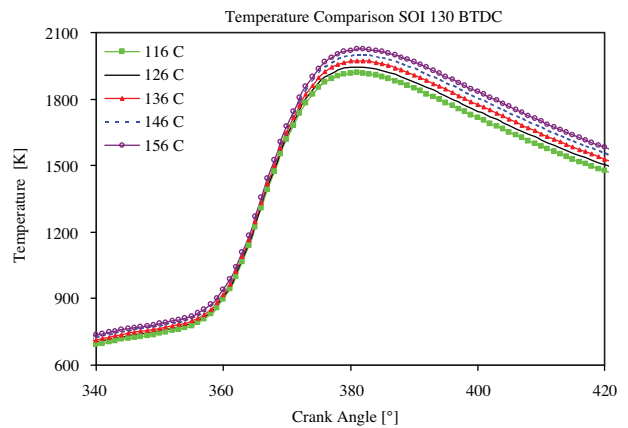


**Figure 6b.** Effect of initial charge temperature on cylinder temperature under injection timing of  $130^\circ$  CA BTDC.

mean and maximum in-cylinder temperature. The effect of increased energy is more important than reduction of the oxygen concentration and, therefore, more  $\text{NO}_x$  emissions are produced.

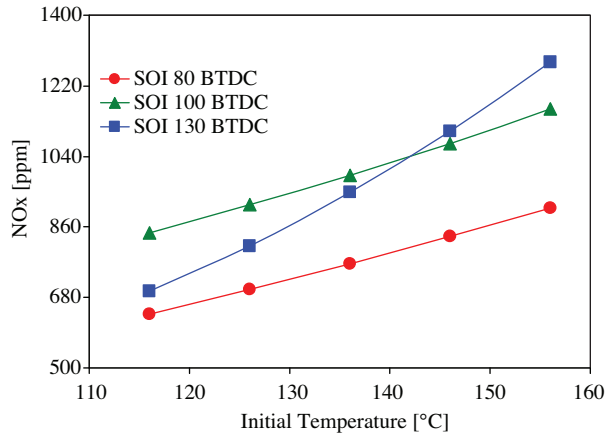


Figure 7.  $\text{NO}_x$  comparison for various initial charge temperatures.

Inhomogeneous mixture formation as a result of retarding the injection timing (late injection) causes incomplete combustion and, therefore, the maximum in-cylinder temperature decreases. The reduction in engine performance also reduces  $\text{NO}_x$  production.

Figures 8 and 9 illustrate the indicated mean effective pressure (IMEP) and indicated specific fuel consumption (ISFC) as a function of initial charge temperature under various injection timings. Because of decreased inlet air mass and therefore in-cylinder pressure as a result of increasing the initial charge temperature, IMEP decreases and ISFC increases. As mentioned above, due to complete combustion by early injection, IMEP increases and ISFC decreases.

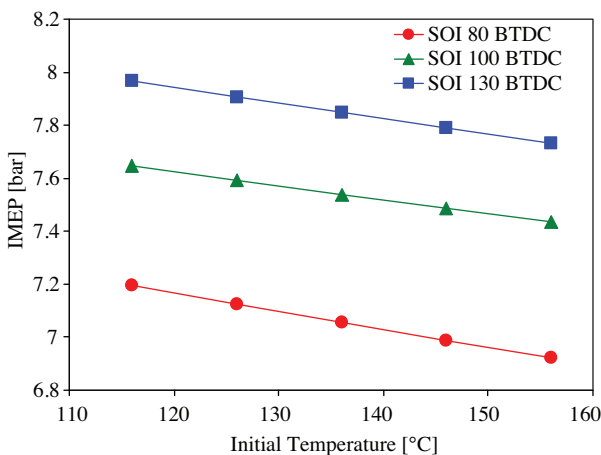


Figure 8. IMEP comparison for various initial charge temperatures.

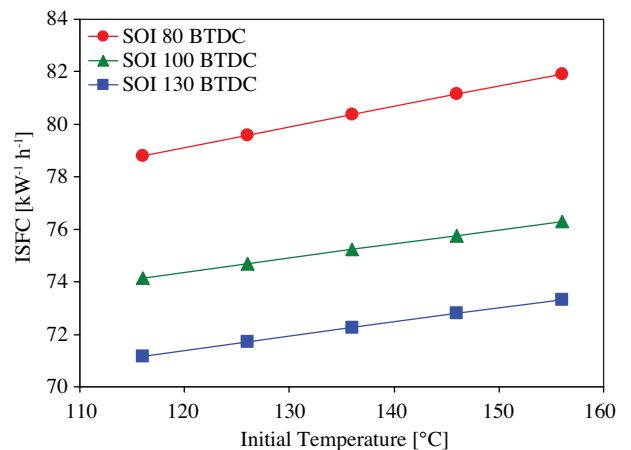


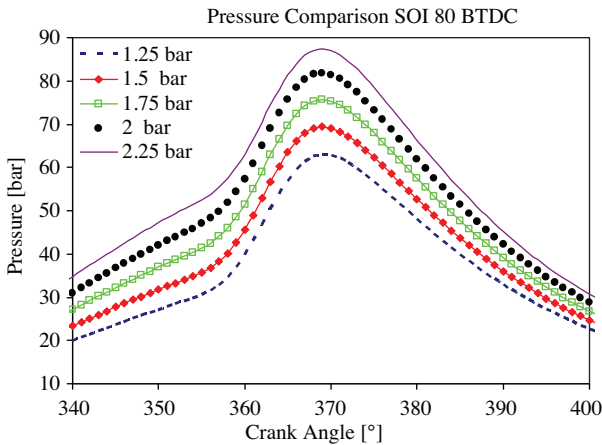
Figure 9. ISFC comparison for various initial charge temperatures.

#### 4.2. Effect of initial charge pressure

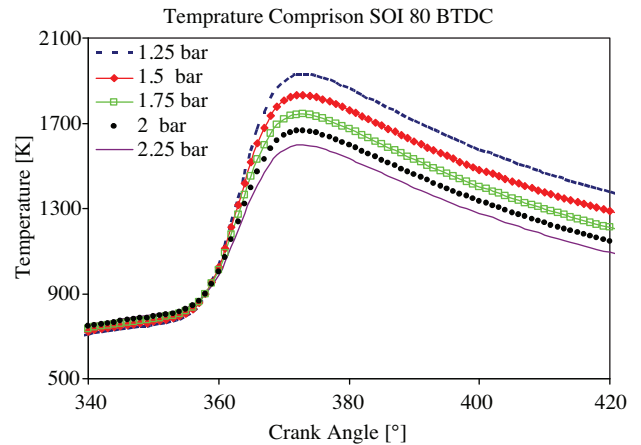
In order to examine the effect of initial charge pressure on the emissions and combustion characteristics, the initial charge pressure was selected to vary between 1.27 and 2.25 bar. Three different injection timings were

used in the simulations and other initial conditions were kept constant as a baseline case.

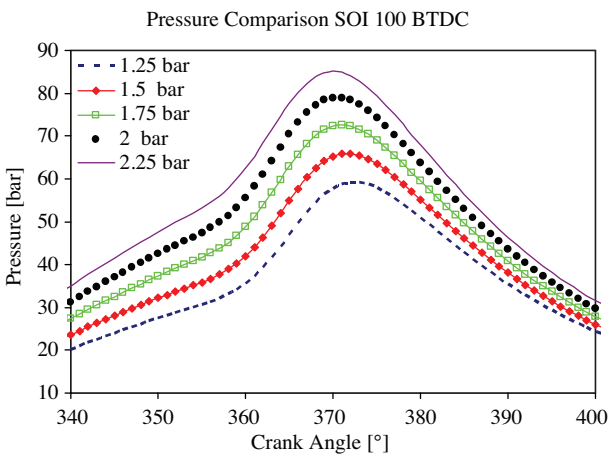
Figures 10a, 10b, 11a, 11b, 12a, and 12b indicate the in-cylinder pressure and temperature at various initial charge pressures. As can be seen, by increasing the initial pressure, the mean and maximum in-cylinder pressure is increased. Figures 10b, 11b, and 12b show that in-cylinder temperature is inversely proportional to the initial charge pressure. This is due to the fact that with the increasing of the initial pressure, the inlet air mass increases; however, the injected hydrogen mass is fixed. This implies that the fuel-air mixture becomes leaner than that at the naturally aspirated condition. Since nonluminous burning will occur in the lean mixture condition, this can explain why the in-cylinder temperature decreases with the increasing of the initial pressure.



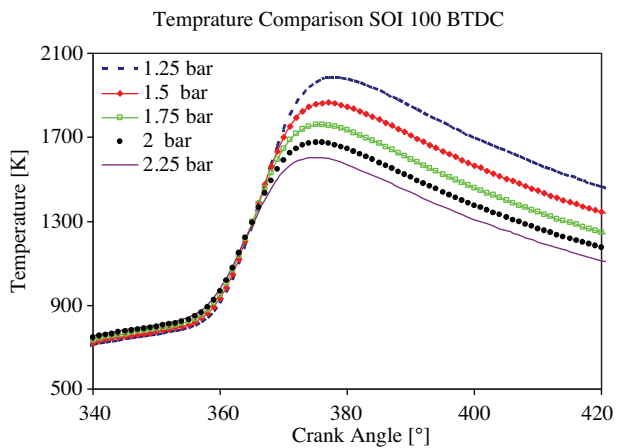
**Figure 10a.** Effect of initial charge pressure on cylinder pressure under injection timing of  $80^\circ$  CA BTDC.



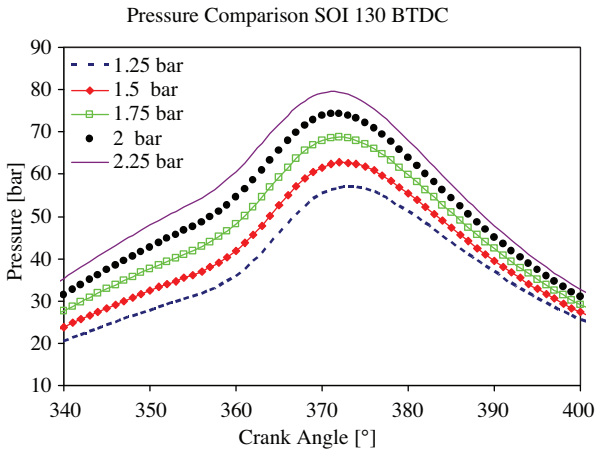
**Figure 10b.** Effect of initial charge pressure on cylinder temperature under injection timing of  $80^\circ$  CA BTDC.



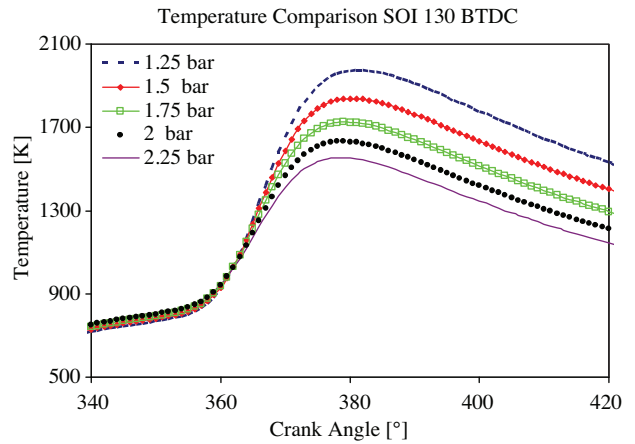
**Figure 11a.** Effect of initial charge pressure on cylinder pressure under injection timing of  $100^\circ$  CA BTDC.



**Figure 11b.** Effect of initial charge pressure on cylinder temperature under injection timing of  $100^\circ$  CA BTDC.



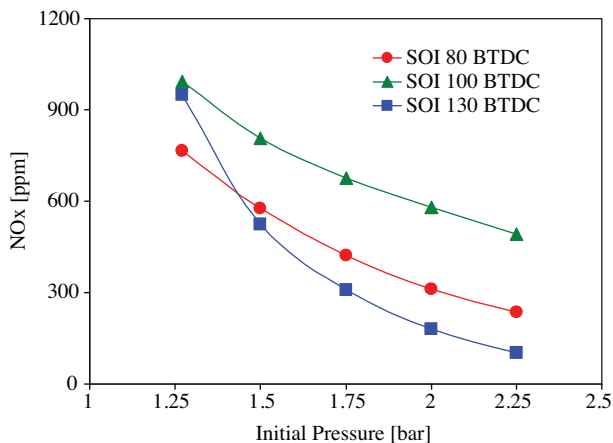
**Figure 12a.** Effect of initial charge pressure on cylinder pressure under injection timing of 130° CA BTDC.



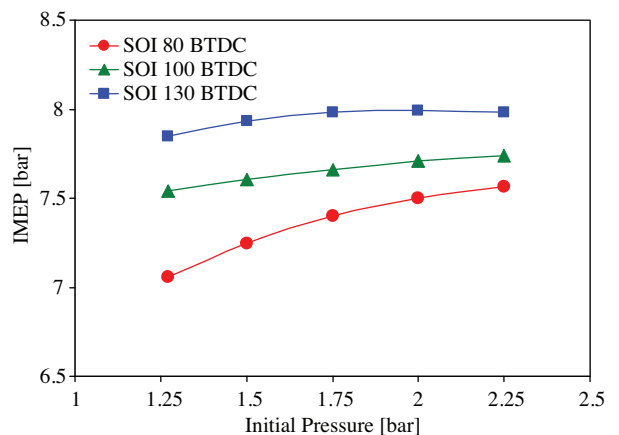
**Figure 12b.** Effect of initial charge pressure on cylinder temperature under injection timing of 130° CA BTDC.

Figure 13 illustrates  $NO_x$  formation under various initial charge pressures at 3 different injection timings. As mentioned before, one effective parameter in  $NO_x$  emission formation is the maximum temperature of the cylinder; by increasing the initial pressure, the in-cylinder temperature decreases, which leads to a reduction of  $NO_x$  emission formation.

By increasing the initial charge pressure, IMEP is increased and ISFC is decreased, as can be seen in Figures 14 and 15. Increasing the initial charge pressure improves performance characteristics such as IMEP and ISFC, and therefore indicates thermal efficiency and reduced  $NO_x$  emission. However, further increases in initial charge pressure decrease the useful life of the engine and may harm the hydrogen injector (Mohammadi et al., 2007).



**Figure 13.**  $NO_x$  comparison for various initial charge pressures.



**Figure 14.** IMEP comparison for various initial charge pressures.

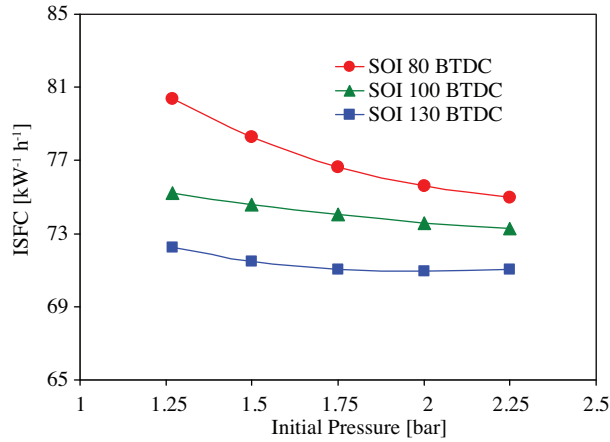


Figure 15. ISFC comparison for various initial charge pressures.

## 5. Conclusion

A numerical investigation was applied to study the effect of the initial charge temperature and initial charge pressure under various hydrogen injection timings in a direct injection spark-ignition hydrogen-fuelled engine at the closed part of the engine cycle. The following general conclusions were drawn from the results of the study:

- Advancing the hydrogen injection timing from 80° to 130° CA BTDC, ISFC was decreased from 80.36 to 72.25 kW<sup>-1</sup> h<sup>-1</sup> and NO<sub>x</sub> emission was increased from 765 to 949 ppm.
- Increasing the initial charge temperature for all injection timings increased ISFC and also increased NO<sub>x</sub> production. The influence of increasing initial temperature on the early hydrogen injection for NO<sub>x</sub> production was greater than other parameters, and thus decreasing initial temperature is a suitable way to improve engine characteristics.
- Boosting initial pressure from 1.25 to 2.25 bar improved ISFC from 72.25 to 71 kW<sup>-1</sup> h<sup>-1</sup>, and NO<sub>x</sub> emission production was reduced from 949 to 101 ppm in the injection timing of 130° CA BTDC. For other injection timings, the same results were obtained.

According to the above results, advancing the hydrogen injection timing has a significant effect on engine performance characteristics such as work, IMEP, ISFC, and the production of NO<sub>x</sub> emissions. By changing initial conditions such as pressure and temperature, optimum engine operating conditions can be found for DISI engines with alternative fuels.

### Nomenclature

$k$  turbulence kinetic energy (m<sup>2</sup> s<sup>-2</sup>)  
 $\varepsilon$  dissipation rate (m<sup>2</sup> s<sup>-2</sup>)  
 $T$  temperature  
 $p$  pressure

$C_{fu}$  constant coefficient for fuel in eddy-breakup model  
 $C_{pr}$  constant coefficient for products in eddy-breakup model  
 $\rho$  density (kg m<sup>-3</sup>)  
 $\lambda$  air-to-fuel equivalence ratio

### Greek letters

$\tau_R$  turbulent mixing time scale

### Abbreviations

IMEP indicated mean effective pressure

ISFC	indicated specific fuel consumption	ppm	parts per million
EGR	exhaust gas recirculation	NO <sub>x</sub>	oxides of nitrogen
ATDC	after top dead center	CO <sub>2</sub>	carbon dioxide
BTDC	before top dead center	HC	hydrocarbon
IVC	intake valve closing	H <sub>2</sub>	hydrogen
EVO	exhaust valve opening	DISI	direct injection spark ignition
SOI	start of injection	CFD	computational fluid dynamics
CA	crank angle	RON	research octane number

### References

- AVL FIRE User Manual V. 8.5, 2006 (<https://www.avl.com/fire>).
- Berckmüller, M., Rottengruber, H., Eder, A., Brehm, N., Elsässer, G. and Müller-Alander, G., “Potentials of a Charged SI-Hydrogen Engine”, SAE Technical Paper No. 2003-01-3210, 2003.
- Bray, K.N.C., “Turbulent Flows with Premixed Reactants”, in Topics in Applied Physics, Vol. 44, Turbulent Reacting Flows (eds. Libby, P.A and Williams, F.A.), Springer-Verlag, New York, 115-183, 1980.
- Eichseder, H., Wallner, T., Freymann, R. and Ringler, J., “The Potential of Hydrogen Internal Combustion Engines in a Future Mobility Scenario”, SAE Paper No. 2003-01-2267, 2003.
- Han, Z. and Reits, R.D., “Turbulence Modeling of Internal Combustion Engine Using RNG  $k-\varepsilon$  Models”, Combustion Science and Technology, 106, 267-295, 1995.
- Kaiser, S.A. and White, C.M., “PIV and PLIF to Evaluate Mixture Formation in a Direct Injection Hydrogen-Fueled Engine”, SAE Paper No. 2008-01-1034, 2008.
- Kirchweger, W., Eichseder, H., Gerbig, F. and Gerke, U., “Optical Measurement Methods for the Optimization of the Hydrogen DI Combustion”, 7th International Symposium on Internal Combustion Engines Diagnostics, Baden-Baden, Germany, 2006.
- Kovac, G., Wimmer, A., Hallmannsegger, M. and Obieglo, A., “Mixture Formation and Combustion in a Hydrogen Engine - A Challenge for the Numerical Simulation”, International Congress on Engine Combustion Processes, Current Problems and Modern Techniques, Munich, Germany, 2005.
- Mohammadi, A., Shioji, M., Nakai, Y., Ishikura, W. and Tabo, E., “Performance and Combustion Characteristics of a Direct Injection SI Hydrogen Engine”, International Journal of Hydrogen Energy, 32, 296-304, 2007.
- Natkin, R.J., Tang, X., Boyer, B., Oltmans, B., Denlinger, A. and Heffel, J.W., “Hydrogen IC Engine Boosting Performance and NO<sub>x</sub> Study”, SAE Technical Paper No. 2003-01-0631, 2003.
- Rahman, M.M., Noor, M.M., Kadirgama, K. and Rejab, M.R.M., “Study of Air Fuel Ratio on Engine Performance of Direct Injection Hydrogen Fueled Engine”, European Journal of Scientific Research, 34, 506-513, 2009.
- Room, J., “The Car and Fuel of the Future”, Energy Policy, 34, 2609-2614, 2006.
- Salazar, V.M., Kaiser, S.A., Nande, A.M. and Wallner T., “The Influence of Injector Position and Geometry on Mixture Preparation in a DI Hydrogen Engine”, 9th International Congress, Engine Combustion Process – Current Problems and Modern Technologies, Munich, Germany, 2009.
- Sierens, R., Verhelst, S. and Verstraeten, S., “An Overview of Hydrogen Fuelled Internal Combustion Engines”, Proceedings of International Hydrogen Energy Congress and Exhibition, İstanbul, Turkey, 2005.
- Tang, X., Kabat, D.M., Natkin, R.J., Stockhausen, W.F. and Heffel, J.W., “Ford P200 Hydrogen Engine Dynamometer Development”, SAE Paper No. 2002-01-0242, 2002.

Verhelst, S., Maesschalck, P., Rombaut, N. and Sierens, R., "Increasing the Power Output of Hydrogen Internal Combustion Engines by Means of Supercharging and Exhaust Gas Recirculation", *International Journal of Hydrogen Energy* 34, 4406-4412, 2009.

Verhelst, S., Sierens, R. and Verstraeten, S., "A Critical Review of Experimental Research on Hydrogen Fueled SI Engines", SAE Paper No. 2006-01-0430, 2006.

Verhelst, S. and Wallner, T., "Hydrogen-Fueled Internal Combustion Engines", *Progress in Energy and Combustion Science*, 35, 490-527, 2009.

Wallner, T., Ciatti, S. and Bihari, B., "Investigation of Injection Parameters in a Hydrogen DI Engine Using an Endoscopic Access to the Combustion Chamber", SAE Paper No. 2007-01-1464, 2007.

Wallner, T., Ciatti, S., Bihari, B., Stockhausen, W. and Boyer, B., "Endoscopic Investigations in a Hydrogen Internal Combustion Engine", *Proceedings of 1st International Symposium on Hydrogen Internal Combustion Engines*, Graz, Austria, 107-117, 2006.

Wallner, T., Nande, A. and Naber, J., "Study of Basic Injection Configurations Using a Direct-Injection Hydrogen Research Engine", SAE Paper No, 2009-01-1418, 2009.

Zeldovich, Y.B., Sadovnikov, P.Y. and Kamenetskii, D.A.F., "Oxidation of Nitrogen in Combustion" (translated by M. Shelef), *Academy of Sciences of USSR, Institute of Chemical Physics, Moscow-Leningrad*, 1974.